

Semiclassical Description of Radiative Decay in a Colored Vacuum

20 March 2002

Prepared by

J. C. CAMPARO
Electronics and Photonics Laboratory
Laboratory Operations

Prepared for

SPACE AND MISSILE SYSTEMS CENTER
AIR FORCE SPACE COMMAND
2430 E. El Segundo Boulevard
Los Angeles Air Force Base, CA 90245

20020422 240

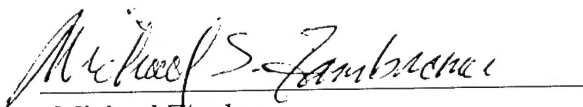
Engineering and Technology Group

APPROVED FOR PUBLIC RELEASE;
DISTRIBUTION UNLIMITED

This report was submitted by The Aerospace Corporation, El Segundo, CA 90245-4691, under Contract No. F04701-00-C-0009 with the Space and Missile Systems Center, 2430 E. El Segundo Blvd., Los Angeles Air Force Base, CA 90245. It was reviewed and approved for The Aerospace Corporation by B. Jaduszliwer, Principal Director, Electronics and Photonics Laboratory. Michael Zambrana was the project officer for the Mission-Oriented Investigation and Experimentation (MOIE) program.

This report has been reviewed by the Public Affairs Office (PAS) and is releasable to the National Technical Information Service (NTIS). At NTIS, it will be available to the general public, including foreign nationals.

This technical report has been reviewed and is approved for publication. Publication of this report does not constitute Air Force approval of the report's findings or conclusions. It is published only for the exchange and stimulation of ideas.


Michael Zambrana
SMC/AXE

REPORT DOCUMENTATION PAGE				Form Approved OMB No. 0704-0188	
Public reporting burden for this collection of information is estimated to average 1 hour per response, including the time for reviewing instructions, searching existing data sources, gathering and maintaining the data needed, and completing and reviewing this collection of information. Send comments regarding this burden estimate or any other aspect of this collection of information, including suggestions for reducing this burden to Department of Defense, Washington Headquarters Services, Directorate for Information Operations and Reports (0704-0188), 1215 Jefferson Davis Highway, Suite 1204, Arlington, VA 22202-4302. Respondents should be aware that notwithstanding any other provision of law, no person shall be subject to any penalty for failing to comply with a collection of information if it does not display a currently valid OMB control number. PLEASE DO NOT RETURN YOUR FORM TO THE ABOVE ADDRESS.					
1. REPORT DATE (DD-MM-YYYY) 20-03-2002		2. REPORT TYPE		3. DATES COVERED (From - To)	
4. TITLE AND SUBTITLE Semiclassical Description of Radiative Decay in a Colored Vacuum				5a. CONTRACT NUMBER F04701-00-C-0009	
				5b. GRANT NUMBER	
				5c. PROGRAM ELEMENT NUMBER	
6. AUTHOR(S) J. C. Camparo				5d. PROJECT NUMBER	
				5e. TASK NUMBER	
				5f. WORK UNIT NUMBER	
7. PERFORMING ORGANIZATION NAME(S) AND ADDRESS(ES) The Aerospace Corporation Laboratory Operations El Segundo, CA 90245-4691				8. PERFORMING ORGANIZATION REPORT NUMBER TR-99(8555)-10	
9. SPONSORING / MONITORING AGENCY NAME(S) AND ADDRESS(ES) Space and Missile Systems Center Air Force Space Command 2450 E. El Segundo Blvd. Los Angeles Air Force Base, CA 90245				10. SPONSOR/MONITOR'S ACRONYM(S) SMC	
				11. SPONSOR/MONITOR'S REPORT NUMBER(S) SMC-TR-02-19	
12. DISTRIBUTION/AVAILABILITY STATEMENT Approved for public release; distribution unlimited.					
13. SUPPLEMENTARY NOTES					
14. ABSTRACT Recently, there has been considerable interest in atoms confined to optical cavities or embedded within photonic band-gap materials, where the spectrum of vacuum fluctuations is modified. As a first step in extending traditional semiclassical methods into this regime, the present paper describes a semiclassical, density-matrix methodology for treating radiative processes in a low-Q cavity. This semiclassical approach is tested by comparing its predictions to the optical cavity experiments of Heinzen and Feld [Phys. Rev. Lett. 59, 2623 (1987)] and by calculating transient-nutation decay in free space induced by a broadband laser. The methodology is then used to examine transient nutation in a low-Q optical cavity, where it is found that the detuning between the atomic and cavity resonances has a significant effect on the transient nutation's decay rate.					
15. SUBJECT TERMS Quantum electrodynamics, Cavity QED, Lasers, Photonic bandgaps					
16. SECURITY CLASSIFICATION OF:			17. LIMITATION OF ABSTRACT	18. NUMBER OF PAGES 12	19a. NAME OF RESPONSIBLE PERSON James Camparo
a. REPORT UNCLASSIFIED	b. ABSTRACT UNCLASSIFIED	c. THIS PAGE UNCLASSIFIED			19b. TELEPHONE NUMBER (include area code) (310)336-6944

Note

The material reproduced in this report originally appeared in *Physical Review A*. The TR is published to document the work for the corporate record.

Physical Review A, Vol. 65, 013815. © 2001 The American Physical Society.

Semiclassical description of radiative decay in a colored vacuum

James Camparo

Department of Physics, California State University Dominguez Hills, 1000 E. Victoria Street, Carson, California 90747
and Electronics and Photonics Laboratory, The Aerospace Corporation, P.O. Box 92957, Los Angeles, California 90009

(Received 23 January 2001; published 14 December 2001)

Recently, there has been considerable interest in atoms confined to optical cavities or embedded within photonic band-gap materials, where the spectrum of vacuum fluctuations is modified. As a first step in extending traditional semiclassical methods into this regime, the present paper describes a semiclassical density-matrix methodology for treating radiative processes in a low- Q cavity. This semiclassical approach is tested by comparing its predictions to the optical cavity experiments of Heinzen and Feld [Phys. Rev. Lett. **59**, 2623 (1987)] and by calculating transient-nutation decay in free space induced by a broadband laser. The methodology is then used to examine transient nutation in a low- Q optical cavity, where it is found that the detuning between the atomic and cavity resonances has a significant effect on the transient nutation's decay rate.

DOI: 10.1103/PhysRevA.65.013815

PACS number(s): 42.50.Lc, 03.65.Sq, 32.80.-t

I. INTRODUCTION

Although the semiclassical description of radiative processes is only a surrogate for quantum electrodynamics, semiclassical methods nonetheless remain a vital tool for studying field/atom interactions [1]. In particular, processes ranging from magnetic resonance [2] to optical pumping [3] to multiphoton ionization [4] are all well described using the semiclassical density matrix. Notwithstanding their present utility, however, semiclassical methods typically limit themselves to situations in which a simple spontaneous-emission-decay term may be added to the appropriate equations in the fashion of a Weisskopf-Wigner approximation [5]. While this procedure is valid for treating spontaneous emission in free space, since the correlation time of vacuum fluctuations in that case is infinitely short; it is at best problematic, and generally just wrong, when considering radiative processes in cavities or photonic bandgap materials where the atom's vacuum environment is modified.

With the growing interest in radiative processes taking place within structured vacuum environments [6], it seems only natural to attempt an extension of semiclassical methods into this regime. For example, given recent demonstrations of lasing in photonic band gaps [7], there could be value in describing photonic band-gap lasers by using standard, semiclassical laser theory [8]. Additionally, with an eye on atomic clock applications, fully semiclassical methods could be used advantageously to describe the dynamics of atoms confined in high- Q optical cavities. Towards the eventual goal of developing these computational techniques, the present work incorporates a semiclassical treatment of spontaneous emission into the density-matrix equations in order to obtain a completely semiclassical methodology for describing radiative processes in a colored vacuum (i.e., a low- Q cavity). The principal question to be addressed here is whether or not such a semiclassical approach is viable given the serious problems encountered in previous attempts [9].

The difficulty with the present program is that spontaneous emission is fundamentally different from other relaxation processes [10], since transitions are only allowed from higher to lower energy eigenstates. This "microscopic re-

versibility issue" is a major obstacle to all semiclassical theories of spontaneous emission [11], and in the present work we circumvent the problem by attributing spontaneous decay to two complementary Hermitian processes. For the first of these processes, the vacuum of QED is approximated by a classical zero-point field (zpf) [12], which induces dipole transitions between atomic states. Additionally, so as to retain consistency with QED [13], we assume that the atom's interaction with the zpf causes it to emit a radiation-reaction field, which also induces dipole transitions. For higher-energy to lower-energy atomic transitions these two pathways add constructively to produce spontaneous decay, while in the case of lower- to higher-energy transitions the two pathways destructively interfere, eliminating any possibility of "spontaneous excitation" [14].

In what follows, the density-matrix equations are obtained by averaging over the zero-point field and by assuming that the atom does not modify the zpf spectrum. This latter assumption restricts the present theory to situations where the correlation time associated with vacuum fluctuations is shorter than the atom's excited-state lifetime. The resulting density-matrix equations are therefore reminiscent of a master-equation-type approach to the problem, where the equations are obtained by tracing over reservoir states [15]. However, the Markov approximation is not invoked, so that in the case of strong fields the Rabi period can be equal to or smaller than the zpf correlation time.

Following a derivation of the density-matrix equations in Sec. II, the semiclassical approach is tested in Sec. III by comparing its predictions of spontaneous emission and the Lamb shift in an optical cavity to the measurements of Heinzen and Feld [16]. The strong-field manifestation of the theory is then examined by computing an atomic population's transient-nutation decay in free space. In order to make this test a bit more difficult, we consider a situation in which the nutation is induced by a stochastic laser field (i.e., a phase-diffusion field), and then compare our results to well-established expectations. Finally, in Sec. IV transient nutation in a colored vacuum is examined, and it is shown that the transient-nutation decay rate is strongly dependent on the detuning between the cavity and atomic resonances. While

this latter result is new, it is nonetheless consistent with the findings of Keitel *et al.* [17], who employed QED to examine resonance fluorescence in a colored vacuum.

II. DENSITY-MATRIX EQUATIONS

A. Semiclassical spontaneous emission

For simplicity, we consider a two-level atom, where $|1\rangle$ is the ground state and $|2\rangle$ the excited state, and the energy separation between the two levels is $\hbar\omega_{21}$. The perturbation acting on the atom is made up of three Hermitian terms: V^L , the perturbation due to dipole coupling between the atom and some real (e.g., laser) field; V^0 , the perturbation due to dipole coupling between the atom and the classical zero-point-field construct; and V^{RR} , the perturbation arising from the atom's interaction with its own radiation-reaction (RR) field [18]. Thus, we write the Liouville equation for the atom's density matrix in the interaction picture σ as

$$\dot{\sigma} = -\frac{i}{\hbar}[(V_I^L + V_I^0 + V_I^{RR}), \sigma] = \dot{\sigma}^L + \dot{\sigma}^0 + \dot{\sigma}^{RR}, \quad (1)$$

where $V_I \equiv e^{iH_0 t/\hbar} V e^{-iH_0 t/\hbar}$ and H_0 is the unperturbed atomic Hamiltonian. We note that by associating the vacuum and radiation-reaction fields with Hermitian operators in Eq. (1), we are in effect following a prescription of Dalibard, Dupont-Roc, and Cohen-Tannoudji [19]. These authors suggest that even though any ordering of creation/annihilation operators is valid in QED, a symmetric ordering provides the greatest physical meaning, since vacuum fluctuation and radiation-reaction terms in QED are then separately Hermitian. Such an ordering attributes one half of an atom's spontaneous decay rate to interaction with the vacuum and the other half to interaction with the radiation-reaction field, similar to what is indicated by Eq. (1).

Density-matrix evolution due to the real field is, of course, well known and leads in the rotating-wave approximation to the standard radiative equations without relaxation terms:

$$\dot{\sigma}_{22}^L = -\Omega \text{Im}[\sigma_{12} e^{-i\Delta_L t}], \quad (2a)$$

$$\dot{\sigma}_{12}^L = \frac{i\Omega}{2} e^{i\Delta_L t} (2\sigma_{22} - 1). \quad (2b)$$

Here, and in what follows, we consider the real field as arising from a linearly polarized laser, so that Δ_L is the detuning between the laser and the atomic resonance (i.e., $\omega - \omega_{21}$); Ω is the Rabi frequency associated with the laser/atom interaction, and the diagonal components of the density matrix have been normalized. Note that the atom's interaction with the real field defines a quantization axis for the atoms that we take as the x axis of our coordinate system.

Turning to the atom's interaction with the zero-point field, the zpf electric field component \bar{E}^0 , is written as a sum over modes s and polarizations λ [14]:

$$\bar{E}^0 = i \left(\frac{\pi\hbar}{L^3} \right)^{1/2} \sum_{s\lambda} C_s \hat{\epsilon}_{s\lambda} \sqrt{\omega_s} \times [z_{s\lambda} \exp(-i\omega_s t) - z_{s\lambda}^* \exp(i\omega_s t)], \quad (3)$$

where L is some large volume (eventually representing free space and not the volume of some experimental optical cavity), $\hat{\epsilon}_{s\lambda}$ is a polarization vector, ω_s is the frequency of the s th mode, and the $z_{s\lambda}$ are independent, mean zero, complex random variables: $\langle z_{s\lambda} z_{r\mu} \rangle = \langle z_{s\lambda}^* z_{r\mu}^* \rangle = 0$ and $\langle z_{s\lambda} z_{r\mu}^* \rangle = \delta_{sr} \delta_{\lambda\mu}$ [14]. C_s is a relative modal amplitude for the zpf associated with its coloring by an optical cavity as will be discussed more fully below.

As mentioned above, the atomic dipole moment $\bar{\mu}$ is oriented in space due to the atom's interaction with the laser field. Thus, the zpf perturbation on the atom becomes

$$\begin{aligned} V_{\alpha\beta}^0 &= -\langle \alpha | \bar{\mu} \cdot \bar{E}^0 | \beta \rangle \\ &= -i\mu_{\alpha\beta} \left(\frac{\pi\hbar}{L^3} \right)^{1/2} \sum_{s\lambda} C_s (\hat{x} \cdot \hat{\epsilon}_{s\lambda}) \\ &\quad \times \sqrt{\omega_s} [z_{s\lambda} \exp(-i\omega_s t) - z_{s\lambda}^* \exp(i\omega_s t)]. \end{aligned} \quad (4)$$

In standard fashion, Eq. (4) may be employed in the Liouville equation in order to obtain

$$\begin{aligned} \dot{\sigma}_{22}^0 &= -2|\mu_{21}| \left(\frac{\pi}{\hbar L^3} \right)^{1/2} \sum_{s\lambda} C_s (\hat{x} \cdot \hat{\epsilon}_{s\lambda}) \sqrt{\omega_s} \\ &\quad \times \text{Re}\{\sigma_{12} z_{s\lambda} \exp(-i\delta_s t)\} \end{aligned} \quad (5)$$

for the evolution of the excited-state density-matrix element, where $\delta_s \equiv (\omega_s - \omega_{21})$, and

$$\begin{aligned} \dot{\sigma}_{12}^0 &= -|\mu_{21}| \left(\frac{\pi}{\hbar L^3} \right)^{1/2} \sum_{s\lambda} C_s (\hat{x} \cdot \hat{\epsilon}_{s\lambda}) \sqrt{\omega_s} z_{s\lambda}^* \\ &\quad \times \exp(i\delta_s t) (\sigma_{11} - \sigma_{22}) \end{aligned} \quad (6)$$

for the coherence term of the density matrix. Note that in writing Eqs. (5) and (6), rapidly rotating terms have been ignored as they effectively average to zero over the time scale for density-matrix evolution.

Proceeding to the radiation-reaction field's contribution to the evolution of the density matrix, we have $V^{RR} = -\bar{\mu} \cdot \bar{E}^{RR}$. Here, \bar{E}^{RR} is the radiation-reaction field emitted by the atom, which almost by definition is an atomic operator. In Ref. [14], the radiation-reaction field was written as an Hermitian operator,

$$\bar{E}^{RR} = \frac{i}{3\hbar^3 c^3} (\bar{\mu} H_0^3 - H_0^3 \bar{\mu}). \quad (7)$$

Though this particular expression for \bar{E}^{RR} leads to a non-Hermitian perturbation, so that some modified form would be required in the present analysis, it is important to note that the radiation-reaction field operator of Eq. (7) is *not* gauge invariant [20]. This may be immediately recognized through the field's dependence on H_0 [21]. Thus, even though each of

the terms in Eq. (1) has a clear physical interpretation (since they are all Hermitian), this interpretation would seem to depend on the choice of gauge.

Though one might be tempted to view the gauge dependence of the radiation-reaction field as problematic for the present semiclassical approach, in actuality it should be seen as a *requirement* for its consistency with QED. Since vacuum fluctuations and radiation reaction are really just "two sides of the same coin" in quantum electrodynamics [13], any appearance of separability between the vacuum and radiation-reaction fields must be illusory. In the present semiclassical approach, this manifests itself as a gauge dependence of \vec{E}^{RR} . Thus, there is no radiation-reaction field that exists independently of the vacuum in the semiclassical approach: it is only the present choice of gauge that allows for such an interpretation.

Since \vec{E}^{RR} (and hence V^{RR}) is not gauge invariant, it is not a measurable quantity; it is simply a computational tool [20]. Thus, while we could attempt to devise a colored vacuum analog to Eq. (7), and then compute the perturbation's matrix elements as was done above for the zpf, there is really no point using that procedure if a more expedient approach may be found. Here, we take advantage of the fact that *on average* radiation reaction and the zpf must constructively interfere to produce excited-state decay, while they must destructively interfere to inhibit spontaneous excitation of the ground state [14,22]. Specifically, due to the linearity of density-matrix evolution, we assume that we can write the zpf-averaged evolution of any density-matrix element as

$$\langle \dot{\sigma}_{\alpha\beta}^0 \rangle_{zpf} = \langle f(\sigma_{11}) \rangle + \langle g(\sigma_{22}) \rangle, \quad (8)$$

where f and g are arbitrary functions or linear operators. Then, by appealing to the fluctuation-dissipation theorem [23], we make the ansatz that

$$\langle \dot{\sigma}_{\alpha\beta}^{RR} \rangle = -\langle f(\sigma_{11}) \rangle + \langle g(\sigma_{22}) \rangle \quad (9)$$

so that

$$\langle \dot{\sigma}_{\alpha\beta}^0 \rangle_{zpf} + \langle \dot{\sigma}_{\alpha\beta}^{RR} \rangle = 2\langle g(\sigma_{22}) \rangle. \quad (10)$$

Evidence for Eq. (10) derives from the fact that it has the proper form to describe spontaneous decay in free space [14] and that it is consistent with the QED-derived relationship between radiation reaction and the electromagnetic vacuum [24]. In the present work, we obtain further validation for Eq. (10) *a posteriori*, when we compare the predictions of the semiclassical approach with experiment in Sec. III. (Further discussion of this ansatz is provided in the Appendix.)

Proceeding, Eqs. (5) and (6) are averaged over the $z_{s\lambda}$ yielding

$$\begin{aligned} \langle \dot{\sigma}_{22}^0 \rangle_{zpf} = & -2|\mu_{21}| \left(\frac{\pi}{\hbar L^3} \right)^{1/2} \sum_{s\lambda} C_s(\hat{x} \cdot \hat{\epsilon}_{s\lambda}) \sqrt{\omega_s} \\ & \times \text{Re} \{ \langle \sigma_{12} z_{s\lambda} \rangle_{zpf} \exp(-i\delta_s t) \} \end{aligned} \quad (11a)$$

and

$$\begin{aligned} \langle \dot{\sigma}_{12}^0 \rangle_{zpf} = & -|\mu_{21}| \left(\frac{\pi}{\hbar L^3} \right)^{1/2} \sum_{s\lambda} C_s(\hat{x} \cdot \hat{\epsilon}_{s\lambda}) \sqrt{\omega_s} \exp(i\delta_s t) \\ & \times \langle z_{s\lambda}^* (\sigma_{11} - \sigma_{22}) \rangle_{zpf}. \end{aligned} \quad (11b)$$

(In what follows we will drop the zpf subscript on the angular brackets, it being understood.) Considering for the moment just the coherence term, we immediately obtain from Eq. (10)

$$\begin{aligned} \langle \dot{\sigma}_{12}^0 \rangle + \langle \dot{\sigma}_{12}^{RR} \rangle = & 2|\mu_{21}| \left(\frac{\pi}{\hbar L^3} \right)^{1/2} \sum_{s\lambda} C_s(\hat{x} \cdot \hat{\epsilon}_{s\lambda}) \sqrt{\omega_s} \exp(i\delta_s t) \\ & \times \langle z_{s\lambda}^* \sigma_{22} \rangle. \end{aligned} \quad (12)$$

In order to evaluate the correlation between the zpf and the density matrix in Eq. (12), we recognize from Eq. (1) that

$$\langle z_{s\lambda} \sigma_{\alpha\beta}(t) \rangle = \langle z_{s\lambda} \sigma_{\alpha\beta}(0) \rangle + \int_0^t \langle z_{s\lambda} (\dot{\sigma}^L + \dot{\sigma}^0 + \dot{\sigma}^{RR})_{\alpha\beta} \rangle dt'. \quad (13)$$

In Eq. (13), we first note that the correlation between any single zpf mode and the density matrix should be small, since density-matrix evolution is influenced by a large number of independent zpf modes. Thus, we make a (second-order) decorrelation approximation on the right-hand side of Eq. (13), such that for some function of the zpf random amplitudes $\Psi(z_{s\lambda})$ we have under the integral sign of Eq. (13)

$$\langle \Psi(z_{s\lambda}) \sigma_{\alpha\beta} \rangle \equiv \langle \Psi(z_{s\lambda}) \rangle \langle \sigma_{\alpha\beta} \rangle. \quad (14)$$

We then get from Eqs. (2) and (14) $\langle z_{s\lambda} \dot{\sigma}_{\alpha\beta}^L \rangle \equiv 0$. In this same spirit, we invoke a mean-field approximation with regard to the atom's radiation-reaction field [25], basically assuming that $V^{RR} \equiv \langle V^{RR} \rangle$ due to the large number of zpf modes that contribute to this field. In combination with the decorrelation approximation, this mean-field approximation implies that $\dot{\sigma}_{\alpha\beta}^{RR} \rightarrow \langle \dot{\sigma}_{\alpha\beta}^{RR} \rangle$, so that $\langle z_{s\lambda} \dot{\sigma}_{\alpha\beta}^{RR} \rangle \rightarrow 0$. In this way, the (first-order) correlation between the density-matrix elements and the zpf is given by the atom's direct coupling to the zpf. Thus,

$$\langle z_{s\lambda} \sigma_{\alpha\beta}(t) \rangle \equiv \left\langle z_{s\lambda} \int_0^t \dot{\sigma}_{\alpha\beta}^0 dt' \right\rangle, \quad (15)$$

so that Eq. (12) becomes

$$\begin{aligned} \langle \dot{\sigma}_{12}^0 \rangle + \langle \dot{\sigma}_{12}^{RR} \rangle = & 2|\mu_{21}| \left(\frac{\pi}{\hbar L^3} \right)^{1/2} \sum_{s\lambda} C_s(\hat{x} \cdot \hat{\epsilon}_{s\lambda}) \sqrt{\omega_s} \exp(i\delta_s t) \\ & \times \left\langle z_{s\lambda}^* \int_0^t \dot{\sigma}_{22}^0 dt' \right\rangle. \end{aligned} \quad (16)$$

Using Eq. (5), we are finally led to

$$\begin{aligned} \langle \dot{\sigma}_{12}^0 \rangle + \langle \dot{\sigma}_{12}^{RR} \rangle = & -\frac{2\pi}{\hbar L^3} |\mu_{21}|^2 \sum_{s\lambda} C_s^2 (\hat{x} \cdot \hat{\epsilon}_{s\lambda})^2 \omega_s \\ & \times \int_0^t \langle \sigma_{12}(t') \rangle \exp[i\delta_s(t-t')] dt'. \end{aligned} \quad (17)$$

Employing a similar line of argument for Eq. (11a), we obtain

$$\begin{aligned} \langle \dot{\sigma}_{22}^0 \rangle = & -2|\mu_{21}|^2 \left(\frac{\pi}{\hbar L^3} \right)^{1/2} \sum_{s\lambda} C_s (\hat{x} \cdot \hat{\epsilon}_{s\lambda}) \sqrt{\omega_s} \\ & \times \text{Re} \left\{ \exp(-i\delta_s t) \left\langle \sigma_{22} \int_0^t \dot{\sigma}_{12}(t') dt' \right\rangle \right\}, \end{aligned} \quad (18)$$

which with the aid of Eq. (6) becomes

$$\begin{aligned} \langle \dot{\sigma}_{22}^0 \rangle = & \frac{2\pi}{\hbar L^3} |\mu_{21}|^2 \sum_{s\lambda} C_s^2 (\hat{x} \cdot \hat{\epsilon}_{s\lambda})^2 \omega_s \\ & \times \int_0^t [\langle \sigma_{11}(t') \rangle - \langle \sigma_{22}(t') \rangle] \cos[\delta_s(t-t')] dt'. \end{aligned} \quad (19)$$

Then, employing Eq. (10), we obtain

$$\begin{aligned} \langle \dot{\sigma}_{22}^0 \rangle + \langle \dot{\sigma}_{22}^{RR} \rangle = & -\frac{4\pi}{\hbar L^3} |\mu_{21}|^2 \sum_{s\lambda} C_s^2 (\hat{x} \cdot \hat{\epsilon}_{s\lambda})^2 \omega_s \\ & \times \int_0^t \langle \sigma_{22}(t') \rangle \cos[\delta_s(t-t')] dt'. \end{aligned} \quad (20)$$

For the numerical computations to follow, it will be more convenient to express the length L appearing in Eqs. (17) and (20) in terms of a zpf-mode spacing $\Delta\omega_s$. Thus, since $L^3 = 2\pi^2 c^3 / \omega_s^2 \Delta\omega_s$, these two equations become

$$\begin{aligned} \langle \dot{\sigma}_{12}^0 \rangle + \langle \dot{\sigma}_{12}^{RR} \rangle = & -\frac{\omega_{21}^2 \Delta\omega_s}{\pi \hbar c^3} |\mu_{21}|^2 \sum_{s\lambda} C_s^2 (\hat{x} \cdot \hat{\epsilon}_{s\lambda})^2 \omega_s \\ & \times \int_0^t \langle \sigma_{12}(t') \rangle \exp[i\delta_s(t-t')] dt', \end{aligned} \quad (21a)$$

$$\begin{aligned} \langle \dot{\sigma}_{22}^0 \rangle + \langle \dot{\sigma}_{22}^{RR} \rangle = & -\frac{2\omega_{21}^2 \Delta\omega_s}{\pi \hbar c^3} |\mu_{21}|^2 \sum_{s\lambda} C_s^2 (\hat{x} \cdot \hat{\epsilon}_{s\lambda})^2 \omega_s \\ & \times \int_0^t \langle \sigma_{22}(t') \rangle \cos[\delta_s(t-t')] dt'. \end{aligned} \quad (21b)$$

B. Colored vacuum

In order to employ Eqs. (21), some account must be given of the vacuum environment in which the atoms find themselves. Specifically, the C_s and $(\hat{x} \cdot \hat{\epsilon}_{s\lambda})$ must be evaluated. Here, as illustrated in Fig. 1, we restrict our attention to an

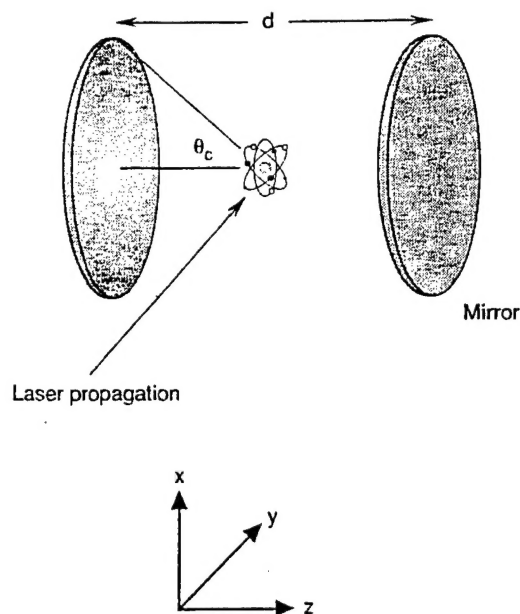


FIG. 1. Illustration showing cavity geometry and coordinate axes.

ensemble of atoms placed in the center of a confocal Fabry-Perot étalon. Remembering that in the present approximation to QED, the zpf is a real field, it is fairly straightforward to describe the effect of the cavity on the zpf: as the cavity is assembled, some of the zpf modes of free space suffer constructive and destructive interference as they reflect off the mirror surfaces. For those modes with $|\cos(\theta_s)| \geq \cos(\theta_c)$, where θ_s is the polar angle for the s th mode's wave vector and θ_c is a critical angle associated with the cavity geometry, it is straightforward to show that

$$\frac{1}{C_s} = (1-R) \left\{ 1 + \left[\frac{4R}{(1-R)^2} \right] \sin^2 \left(\frac{\omega_s d}{c} \right) \right\}^{1/2} \equiv \frac{1}{\kappa_s}. \quad (22)$$

Here, R is the mirror reflectivity and d is the cavity length. Alternatively, C_s equals unity for the modes with $|\cos(\theta_s)| < \cos(\theta_c)$. The linewidth of the confocal étalon (half width at half maximum) for the field evaluated at the center of the cavity is

$$\Delta\omega_c = \frac{c}{d} \sin^{-1} \left[\frac{(1-R)}{2\sqrt{R}} \right] \quad (23)$$

and its free spectral range is just $c/2d$.

Since the above density-matrix analysis has assumed that the C_s are unrelated to the density-matrix elements (i.e., that the atom's dynamics do not influence the zpf modal amplitudes within the cavity), the present theory requires $\Delta\omega_c / \gamma_{\text{rad}} > 1$, where γ_{rad} is the spontaneous decay rate in the cavity. In other words, the present theory assumes that the time scale for the zpf to reach equilibrium within the cavity is shorter than the time scale for the atom to perturb the zpf by its (real) radiative field. It is to be noted, however, that this is not a fundamental limitation to the present semiclassical

sical approach, as in principle it should be possible to relate the C_s to the atom's dynamics.

To determine $(\hat{x} \cdot \hat{\epsilon}_{s\lambda})$, we consider a cavity orientation as illustrated in Fig. 1, with the cavity axis parallel to \hat{z} so that the laser field does not couple into the étalon. Then, defining \vec{k}_s as the wave vector of the s th zpf mode, we have

$$\begin{aligned} C_s^2(\theta_s) \sum_{\lambda} (\hat{x} \cdot \hat{\epsilon}_{s\lambda})^2 &= C_s^2(\theta_s) \left[1 - \frac{(\hat{x} \cdot \vec{k}_s)^2}{|k_s|^2} \right] \\ &= C_s^2(\theta_s) [1 - \sin^2(\theta_s) \cos^2(\varphi_s)], \end{aligned} \quad (24)$$

where φ_s is the azimuthal angle for the s th mode's wave vector and we have specifically indicated the C_s dependence on θ_s . Averaging Eq. (24) over 4π sr [26],

$$\begin{aligned} \eta_s &\equiv \frac{1}{4\pi} \int C_s^2(\theta) [1 - \sin^2(\theta) \cos^2(\theta)] \sin(\theta) d\theta d\varphi \\ &= \frac{2}{3} \left\{ \kappa_s^2 - \frac{3(\kappa_s^2 - 1)}{4} \left[\cos(\theta_c) + \frac{\cos^3(\theta_c)}{3} \right] \right\}. \end{aligned} \quad (25)$$

Thus, in the colored vacuum of a confocal étalon Eqs. (21) become

$$\begin{aligned} \langle \dot{\sigma}_{12}^0 \rangle + \langle \dot{\sigma}_{12}^{\text{RR}} \rangle &= -\frac{\omega_{21}^2 \Delta \omega_s}{\pi \hbar c^3} |\mu_{21}|^2 \int_0^t \langle \sigma_{12}(t') \rangle \\ &\times \left[\sum_s \eta_s \omega_s \exp[i\delta_s(t-t')] \right] dt' \end{aligned} \quad (26a)$$

and

$$\begin{aligned} \langle \dot{\sigma}_{22}^0 \rangle + \langle \dot{\sigma}_{22}^{\text{RR}} \rangle &= -\frac{2\omega_{21}^2 \Delta \omega_s}{\pi \hbar c^3} |\mu_{21}|^2 \int_0^t \langle \sigma_{22}(t') \rangle \\ &\times \left[\sum_s \eta_s \omega_s \cos[\delta_s(t-t')] \right] dt'. \end{aligned} \quad (26b)$$

C. Numerical considerations for density-matrix computations

To employ Eqs. (26) in a numerical simulation, account must be taken of the discrete time step employed in the simulation and the necessity for employing a finite number of zpf modes. In our paper, we first define a time scale T over which we wish to simulate the atomic dynamics, and then discretize this into elements of length δT . The δT are small enough so that the density-matrix elements do not change significantly over this interval. We then define the two field functions $F_c(t)$ and $F_s(t)$ that are required by Eqs. (26):

$$F_c(t) = \sum_s \eta_s (\omega_{21} + \delta_s) \cos(\delta_s t) \quad (27a)$$

and

$$F_s(t) = \sum_s \eta_s (\omega_{21} + \delta_s) \sin(\delta_s t). \quad (27b)$$

Averaging these over the time step δT , we obtain

$$\bar{F}_c(t) = \sum_s \frac{2\eta_s (\omega_{21} + \delta_s)}{\delta_s \delta T} \sin\left(\frac{\delta_s \delta T}{2}\right) \cos(\delta_s t) \quad (28a)$$

and

$$\bar{F}_s(t) = \sum_s \frac{2\eta_s (\omega_{21} + \delta_s)}{\delta_s \delta T} \sin\left(\frac{\delta_s \delta T}{2}\right) \sin(\delta_s t), \quad (28b)$$

which are the field functions actually employed in the numerical simulations.

The effect of this averaging process is to multiply each of the zpf modes by a sinc function [i.e., $\text{sinc}(x) \equiv \sin(x)/x$], which is just the Fourier transform of the discrete time step employed in the simulation. We can therefore limit the range of modes in the summation by choosing the two values of δ_s where the sinc function has its first zero, since for larger values of $|\delta_s|$ the averaging process causes the modes to have negligible amplitude. Thus, to compute the zpf functions we need only specify the modal spacing $\Delta \omega_s$ and the time step δT , and once computed the zpf functions are incorporated into the density-matrix equations just like any other discretized time function. Simulations are, of course, repeated for various values of $\Delta \omega_s$ and δT to ensure that the results do not depend on the specific numerical parameters.

D. Full density-matrix evolution

Combining Eqs. (2), (26), and (28), we obtain the semiclassical density-matrix equations for the evolution of a two-level atom in the presence of a real (possibly strong) field in a colored vacuum:

$$\begin{aligned} \dot{\sigma}_{22} &= -\Omega \text{Im}[\sigma_{12} e^{-i\Delta_L t}] - \frac{2\omega_{21}^2 \Delta \omega_s}{\pi \hbar c^3} |\mu_{21}|^2 \\ &\times \int_0^t \sigma_{22}(t') \bar{F}_c(t-t') dt' \end{aligned} \quad (29a)$$

and

$$\begin{aligned} \dot{\sigma}_{12} &= \frac{i\Omega}{2} e^{i\Delta_L t} (2\sigma_{22} - 1) - \frac{\omega_{21}^2 \Delta \omega_s}{\pi \hbar c^3} |\mu_{21}|^2 \\ &\times \int_0^t \sigma_{12}(t') [\bar{F}_c(t-t') + i\bar{F}_s(t-t')] dt'. \end{aligned} \quad (29b)$$

(Here, and in what follows, we drop the angular brackets indicating an average over the zpf, this now being understood.) To put these into a more recognizable form, we let $\sigma_{12} \rightarrow \sigma_{12} e^{i\Delta_L t}$, so that

$$\begin{aligned} \dot{\sigma}_{22} &= -\Omega \text{Im}[\sigma_{12}] - \frac{2\omega_{21}^2 \Delta \omega_s}{\pi \hbar c^3} |\mu_{21}|^2 \\ &\times \int_0^t \sigma_{22}(t') \bar{F}_c(t-t') dt' \end{aligned} \quad (30a)$$

and

$$\begin{aligned} \dot{\sigma}_{12} = & -i\Delta_L \sigma_{12} + \frac{i\Omega}{2}(2\sigma_{22} - 1) - \frac{\omega_{21}^2 \Delta \omega_s}{\pi \hbar c^3} |\mu_{21}|^2 \\ & \times \int_0^t \sigma_{12}(t') e^{-i\Delta_L(t-t')} [\bar{F}_c(t-t') + i\bar{F}_s(t-t')] dt'. \end{aligned} \quad (30b)$$

E. Lamb shift

Though it may not be readily apparent, a Lamb-shift term for the two-level atom is included in Eq. (30b). To demonstrate this, we need only compare the first and last terms on the right-hand side of Eq. (30b), thereby recognizing that the imaginary part of the last term must act like a zpf detuning term:

$$\begin{aligned} & -\frac{\omega_{21}^2 \Delta \omega_s}{\pi \hbar c^3} |\mu_{21}|^2 \int_0^t \sigma_{12}(t') \left[\sum_s \eta_s \omega_s \sin[\delta_s(t-t')] \right] dt' \\ & = \sigma_{12} \Delta'_{\text{Lamb}}. \end{aligned} \quad (31)$$

However, in order to obtain a more realistic evaluation of an atom's Lamb shift, specifically a cavity-induced change in the Lamb shift that may be compared to experiment, it is necessary to go beyond the two-level approximation and consider zpf-induced virtual transitions to other atomic states.

Our starting point will be Eq. (32) from Ref. [14], which describes the zpf-induced evolution of an excited-state amplitude, b_m , up to second order in perturbation theory. (The b_m are expansion coefficients of the atomic wave function in terms of its unperturbed basis states, averaged over the zpf.) Specifically,

$$\begin{aligned} \dot{b}_m^0(t) = & -\frac{b_m \Delta \omega_s}{2\pi \hbar c^3} \sum_n |\mu_{mn}|^2 \sum_s \eta_s \omega_s^3 \left[e^{-ik_1 t} \int_0^t e^{ik_1 t'} dt' \right. \\ & \left. + e^{ik_2 t} \int_0^t e^{-ik_2 t'} dt' \right], \end{aligned} \quad (32)$$

where m and n refer to unperturbed energy eigenstates, $k_1 \equiv \omega_s - \omega_{mn}$ and $k_2 \equiv \omega_s + \omega_{nm}$. In writing Eq. (32), the original equation from Ref. [14] has been modified so as to make it applicable to a colored vacuum; it has been averaged over 4π sr, and rapidly oscillating terms in the sum over states have been averaged to zero. Recognizing that the imaginary term of Eq. (32) corresponds to the Lamb shift of $|m\rangle$, Δ_{Lamb} , it is straightforward to show that

$$\begin{aligned} \tilde{\Delta}_{\text{Lamb}} = & \text{Im} \left\{ \frac{\Delta \omega_s}{2\pi \hbar c^3} \sum_{sn}' \eta_s \omega_s^3 |\mu_{mn}|^2 \left[\left(\frac{1 - e^{-ik_1 t}}{ik_1} \right) \right. \right. \\ & \left. \left. - \left(\frac{1 - e^{ik_2 t}}{ik_2} \right) \right] \right\}, \end{aligned} \quad (33)$$

where the prime on the sum indicates that only nonzero terms of k_1 and k_2 are included, as the null values yield real

terms in Eq. (32). In the limit of $t \rightarrow \infty$ and $\Delta \omega_s \rightarrow 0$, the modal sum of the exponential terms in k_1 and k_2 equals zero, so that we have

$$\lim_{t \rightarrow \infty} \tilde{\Delta}_{\text{Lamb}} = \frac{\Delta \omega_s}{\pi \hbar c^3} \sum_{sn}' \eta_s |\mu_{mn}|^2 \left[\frac{\omega_s^3 \omega_{nm}}{\omega_s^2 - \omega_{nm}^2} \right]. \quad (34)$$

To include mass renormalization into Eq. (34) [22], we recognize that in the limit of large-frequency zpf modes,

$$\tilde{\Delta}_{\text{Lamb}} \Rightarrow \frac{\Delta \omega_s}{\pi \hbar c^3} \sum_{sn}' \eta_s |\mu_{mn}|^2 \omega_s \omega_{nm}. \quad (35)$$

Subtracting Eq. (35) from Eq. (34) then yields an expression for the observable Lamb shift of $|m\rangle$,

$$\Delta_{\text{Lamb}} = \frac{\Delta \omega_s}{\pi \hbar c^3} \sum_{sn}' \eta_s |\mu_{mn}|^2 \omega_{nm}^3 \left[\frac{\omega_s}{\omega_s^2 - \omega_{nm}^2} \right]. \quad (36)$$

Though Eq. (36) is logarithmically divergent, and would require a high-frequency cutoff for evaluation, it should be recognized that our interest is not in the Lamb shift itself but in the *change* in the Lamb shift caused by a colored vacuum. We, therefore, define the Lamb shift change δ_{Lamb} as

$$\delta_{\text{Lamb}} \equiv \Delta_{\text{Lamb}}^{\text{cavity}} - \Delta_{\text{Lamb}}^{\text{free space}}. \quad (37)$$

Since $\eta_s = 2/3$ in free space,

$$\delta_{\text{Lamb}}^m = \frac{\Delta \omega_s}{\pi \hbar c^3} \sum_{sn}' \left(\eta_s - \frac{2}{3} \right) |\mu_{mn}|^2 \omega_{nm}^3 \left[\frac{\omega_s}{\omega_s^2 - \omega_{nm}^2} \right], \quad (38)$$

where the superscript on δ_{Lamb} indicates that this value is specific to the energy eigenstate $|m\rangle$. Since the cavity's mirror reflectivity must go to zero for either very low or very high frequency zpf modes, η_s asymptotes to $2/3$ in the high-frequency limit thereby ensuring the convergence of δ_{Lamb} .

In order to evaluate the Lamb shift numerically, we can break the sum over zpf modes into two contributions, those within a cavity-free spectral range of the atom's resonance and those outside this range. For the zpf modes outside the range, we convert the sum over modes to an integral, thereby obtaining

$$\begin{aligned} \delta_{\text{Lamb}}^m = & \frac{1}{\pi \hbar c^3} \sum_n |\mu_{mn}|^2 \omega_{nm}^3 \left\{ \int_{\omega_l}^{\omega_h} L(\omega) d\omega + \sum_{j=1}^N \left(\eta_j - \frac{2}{3} \right) \right. \\ & \left. \times \left[\frac{\omega_j \Delta \omega_s}{\omega_j^2 - \omega_{nm}^2} \right] + \int_{\omega^+}^{\omega_h} L(\omega) d\omega \right\}, \end{aligned} \quad (39)$$

where ω_l and ω_h are the low- and high-frequency cutoffs for the cavity mirror's reflectivity, respectively; ω^- , ω^+ , and $L(\omega)$ are given by

$$\omega^- = \omega_{nm} - \frac{\text{FSR}}{2}, \quad (40a)$$

$$\omega^+ = \omega_{nm} + \frac{\text{FSR}}{2}, \quad (40b)$$

$$L(\omega) = \frac{[\eta(\omega) - \frac{2}{3}]\omega}{\omega^2 - \omega_{nm}^2}, \quad (40c)$$

and

$$\omega_j = \omega^- + j\Delta\omega_s. \quad (41)$$

Note that $\Delta\omega_s$ is to be chosen so that $\omega_j \neq |\omega_{nm}|$.

III. VERIFICATION OF THE SEMICLASSICAL APPROACH

As a first check on the semiclassical description's validity, we compare the predictions of Eqs. (30) and (39) with the experiments of Heinzen and Feld [16], who passed a Ba^{138} beam through an étalon and examined weak-field resonance fluorescence while the atoms were located between the étalon's two concentric mirrors. Heinzen and Feld excited the $6s^2\ ^1S_0$ - $6s6p\ ^1P_1$ transition at 553.5 nm, and recorded the width and central position of the fluorescence. In this way, they were able to obtain both the radiative decay rate of the excited state, γ_{rad} , and the change in the transition's Lamb shift for a quantum system perturbed by a colored vacuum. Their mirror's separation was 5 cm; the mirror diameter was 1.88 cm, and the mirror reflectivities were low. Heinzen and Feld's results are reproduced in Figs. 2(a) and 2(b) as a function of cavity detuning (triangles), where zero detuning implies that the cavity resonance overlaps the atomic resonance. The open circles in Fig. 2(a) correspond to the predictions of Eqs. (30) with $\Omega=0$, based on the cavity geometry and mirror reflectivity parameters provided by Heinzen and Feld [27]. For the theory, it was assumed that at time $t=0$ the atom was in a superposition of the ground state and the excited state, and three decay rates were computed corresponding to the three independent density-matrix elements. In all cases, the coherence and population decays were exponential, and the computed decay rates of the coherence were half that of the population.

The change in the Lamb shift was computed using Eq. (39), where we set $2\pi c/\omega_l = 900\text{ nm}$ and $2\pi c/\omega_h = 350\text{ nm}$. The mirror reflectivity was a constant value between these wavelengths and zero outside this range. The relevant transitions for the Lamb shift calculation are shown in Fig. 3, and the corresponding dipole moments are collected in Table I; the indicated dipole moments come from the Einstein A coefficients of Niggli and Huber [28]. Two theoretical curves are shown in Fig. 2(b). For the solid curve, only the 553.5 nm transition was included in the Lamb shift calculation, while the dashed curve corresponds to inclusion of all transitions shown in Fig. 3. As might have been anticipated based on an examination of the dipole moments, the $6s^2\ ^1S_0$ - $6s6p\ ^1P_1$ transition has the greatest influence on the Lamb shift's change.

The agreement between theory and experiment shown in Figs. 2(a) and 2(b) provides strong evidence for the weak-field validity of the present semiclassical description of ra-

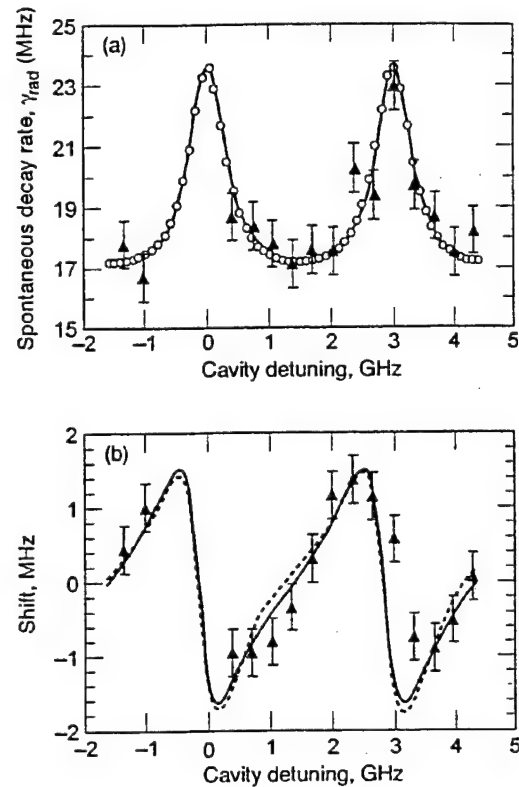


FIG. 2. (a) Spontaneous decay rate in a cavity as a function of cavity tuning. Diamonds correspond to the data of Heinzen and Feld [16], while circles correspond to the present theory. (b) Lamb shift change in the cavity as a function of cavity tuning. Again, diamonds correspond to the data of Heinzen and Feld. For the solid line, only the $6s^2\ ^1S_0$ - $6s6p\ ^1P_1$ transition was included in the Lamb shift computation, while in the case of the dashed line all transitions shown in Fig. 3 were included.

diative decay and the Lamb shift, especially when it is recognized that no free parameters were employed in the density-matrix equations. However, what remains to be assessed is the semiclassical approach's validity in the case of strong field/atom interactions. In this regard, the present theory is most amenable to a computation of transient nutation in a colored vacuum [29]. Unfortunately, no such experiments have been done, at least in cavities conforming to the present theory's limitations on cavity linewidth. Consequently, we have used the present theory to compute transient nutation in free space, and for added rigor have considered nutation induced by a stochastic laser field (i.e., a phase diffusion field or PDF). We compare our results to well-established expectations [30].

For a PDF of linewidth γ_F full width at half maximum, it is well known that the field's phase fluctuations enhance the coherence's relaxation rate while leaving the population relaxation rate unaffected. Specifically, the transient-nutation signal for a two-level atom becomes

$$\sigma_{22}(t) = \sigma_{\infty} \left(1 - \frac{e^{-\Gamma t} \sin(\lambda t + \phi)}{\sin(\phi)} \right), \quad (42)$$

where σ_{∞} corresponds to the steady-state value of the excited-state population. Also,

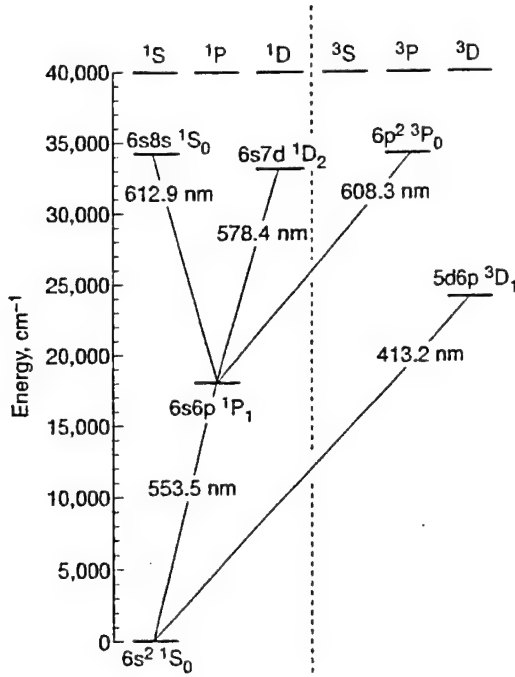


FIG. 3. Partial energy-level diagram of barium.

$$\Gamma = \frac{A_{21} + \gamma_2}{2}, \quad (43a)$$

$$\lambda = \left[\Omega^2 - \left(\frac{\gamma_2 - A_{21}}{2} \right)^2 \right]^{1/2}, \quad (43b)$$

and

$$\phi = \tan^{-1} \left(\frac{\lambda}{\Gamma} \right). \quad (43c)$$

Here, γ_2 corresponds to the coherence decay rate, which according to well-established theory and experiment should equal $(A_{21} + \gamma_F)/2$, and A_{21} is the spontaneous decay rate in free space.

In the test, we again considered laser excitation of the $6s^2 1S_0$ - $6s6p 1P_1$ barium transition. The PDF was numerically simulated for some given value of γ_F and the density-matrix equations were then solved numerically using a variable step-size Runge-Kutta-Fehlberg method [31]. The computed transient-nutation signal was averaged, and then using a nonlinear least squares procedure [32] was fit to Eq.

TABLE I. Selected transition dipole moments for barium. Values are inferred from the lifetime measurements of Niggli and Huber [28].

Transition	Dipole moment, $ \mu $ (esu cm)
$6s6p 1P_1$ - $6s^2 1S_0$	8.0×10^{-18}
$6s8s 1S_0$ - $6s6p 1P_1$	2.1×10^{-18}
$6s7d 1D_2$ - $6s6p 1P_1$	3.6×10^{-18}
$6p^2 3P_0$ - $6s6p 1P_1$	2.8×10^{-18}
$5d6p 3D_1$ - $6s^2 1S_0$	5.8×10^{-19}

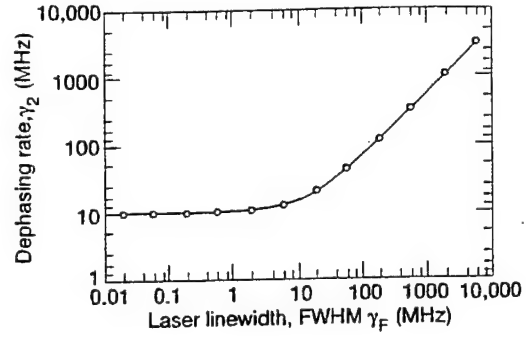


FIG. 4. Atomic dephasing rate in free space as a function of phase-diffusion-field (PDF) linewidth. The solid line corresponds to expectations based on experiment and theory. The open circles correspond to the results of the present theory.

(42) with γ_2 as the one free parameter. The results of the test are shown in Fig. 4 as open circles, where the value of γ_2 from the numerical simulation is plotted as a function of the input value of γ_F . The solid curve in the figure corresponds to the expected value of γ_2 , $(A_{21} + \gamma_F)/2$. The excellent agreement between the numerically simulated value of γ_2 and $(A_{21} + \gamma_F)/2$ not only lends confidence to the present theory's ability to simulate strong field/atom interactions, it also suggests that the semiclassical description of radiative decay may find application in simulating the effects of colored vacua in studies of the stochastic-field/atom interaction.

IV. TRANSIENT NUTATION IN A COLORED VACUUM

Given the previous section's evidence for the validity of the present semiclassical description of radiative decay, we now consider the decay rate of transient nutation in a colored vacuum. For the present study, we confine our attention to a monochromatic laser tuned to barium's $6s^2 1S_0$ - $6s6p 1P_1$ transition, and the cavity geometry of Heinzen and Feld [16]. As discussed above, when the cavity detuning from the atomic resonance Δ_{cav} , equals zero, the population and coherence decay rates in the weak-field limit are at a maximum, with a value determined by the cavity's mirror reflectivity. Consequently, based on Eq. (43a) it was originally thought that the transient-nutation decay rate would be maximized for $\Delta_{\text{cav}} = 0$ with a value of $3\gamma_{\text{rad}}/4$. Using the present work's weak-field results for γ_{rad} , this prediction is shown as the solid line in Fig. 5 as a function of mirror reflectivity.

Transient-nutation decay in a cavity was investigated by numerically solving Eqs. (30a) and (30b) for $\Delta_{\text{cav}} = 0$ using the parameter values listed in Table II. In order to determine the decay rate Γ , we Fourier transformed the transient nutation signal and determined the width of the Fourier spectral component at the nutational frequency. In this way the determination of Γ was independent of any assumption regarding the functional form of the nutation signal in the cavity, as would have been the case had we fit the nutation signal to Eq. (42). The transient-nutation decay rates obtained in this way are shown as circles in Fig. 5. What is strikingly apparent is that the numerical results indicate a decay rate significantly different from the expected $3\gamma_{\text{rad}}/4$ values, and that

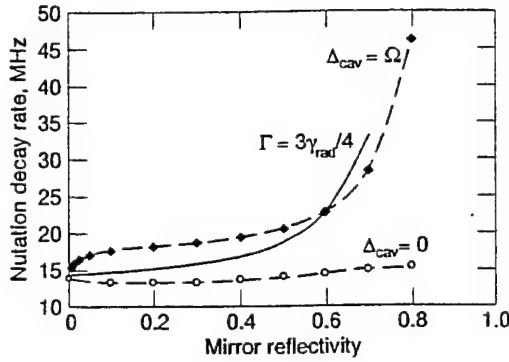


FIG. 5. Transient-nutation decay rate Γ in a cavity as a function of the cavity mirrors' reflectivity. The solid line corresponds to an anticipated value based on the extrapolation of weak-field cavity decay rates into the strong-field regime. Circles correspond to the results of the present theory for $\Delta_{\text{cav}}=0$, while diamonds correspond to the present theory for $\Delta_{\text{cav}}=\Omega$.

for mirror reflectivities less than 0.5 the nutational decay rate is actually less than its free-space value. If the cavity is detuned from the atomic resonance by the Rabi frequency, then the decay rates shown as diamonds in Fig. 5 are obtained. In this case, transient-nutation decay in the cavity is faster than $3\gamma_{\text{rad}}/4$.

To gain a semiquantitative understanding of the nutational decay rate's sensitivity to cavity detuning (and also to highlight the semiclassical approach's intuitive value), we rewrite Eq. (30a) for $t \gg 1/\Delta\omega_c$, so that the upper limit of integration may be replaced by $+\infty$. Moreover, since we are considering nutation, to first approximation we can assume that the strong field causes σ_{22} to oscillate at the Rabi frequency [i.e., $\sigma_{22} = \cos(\Omega t)$]. This then yields

$$\dot{\sigma}_{22} \equiv -\Omega \text{Im}[\sigma_{12}] - \frac{\omega_{21}^2 \Delta\omega_s}{\pi \hbar c^3} |\mu_{21}|^2 \int_{-\infty}^{+\infty} \sigma_{22}(t-\tau) F_c(\tau) d\tau, \quad (44)$$

where the integration variable has been redefined. In this form, the second term on the right-hand side of Eq. (44) has the appearance of a linear system's output [33]; that is, the

TABLE II. Parameters used to compute transient nutation in a colored vacuum.

Parameter	Value
$\sigma_{22}(t=0), \sigma_{12}(t=0)$	0
Resonant wavelength	553.5 nm
Excited-state decay rate in free space, A_{21}	$1.19 \times 10^8 \text{ sec}^{-1}$
Transition dipole moment, $ \mu_{21} $	$8.02 \times 10^{-18} \text{ esu cm}$
Cavity length	5 cm
Mirror diameter	1.88 cm
Laser intensity	100 W/cm^2
Rabi frequency, Ω	$6.97 \times 10^9 \text{ sec}^{-1}$
Laser detuning from atomic resonance, Δ_L	0
Simulation time scale, T	$100/A_{21}$
zpf time-scale discretization, δT	$T/8192$

atom appears to "filter" the vacuum field fluctuations, producing an output that forces the excited state to decay.

Taking advantage of the convolution theorem [33], Eq. (44) can be reexpressed as

$$\dot{\sigma}_{22} \equiv -\Omega \text{Im}[\sigma_{12}] - \frac{\omega_{21}^2 \Delta\omega_s}{2\pi \hbar c^3} |\mu_{21}|^2 \times \int_{-\infty}^{+\infty} \Sigma_{22}(\omega) \Phi_c(\omega) e^{i\omega t} d\omega, \quad (45)$$

where Σ_{22} and Φ_c are the Fourier transforms of σ_{22} and F_c , respectively. Given the oscillatory form of σ_{22} , it is clear that Σ_{22} is a sum of δ functions:

$$\Sigma_{22}(\omega) = \pi[\delta(\Omega - \omega) + \delta(\Omega + \omega)], \quad (46)$$

which on substitution into Eq. (45) and recognizing that $\Phi_c(\omega) = \Phi_c(-\omega)$ yields

$$\dot{\sigma}_{22} \equiv -\Omega \text{Im}[\sigma_{12}] - \bar{\Gamma} \sigma_{22}(t), \quad (47)$$

where

$$\bar{\Gamma} \equiv \frac{\omega_{21}^2 \Delta\omega_s}{\pi \hbar c^3} |\mu_{21}|^2 \Phi_c(\Omega). \quad (48)$$

(Note that in the limit of zero cavity-mirror reflectivity, $\bar{\Gamma} \rightarrow 4\omega_{21}^3 |\mu_{21}|^2 / 3\hbar c^3$, the Einstein A coefficient for $|2\rangle$ to $|1\rangle$ spontaneous decay in free space.)

Thus in the semiclassical approach, the nutational decay rate in a colored vacuum is seen to arise from an "atomic filtering" of the vacuum field fluctuations, with the atom responding principally to that Fourier frequency component of the vacuum's fluctuations corresponding to the Rabi frequency. When the cavity is tuned to the atomic resonance, $\Phi_c(\Omega)$ and hence $\bar{\Gamma}$ can be relatively small. However, when the cavity is detuned from resonance by the Rabi frequency, $\Phi_c(\Omega)$ is at its maximum value and nutational decay is rapid. It is to be noted that this conclusion is consistent with the works of Keitel *et al.* [17] and Lewenstein, Mossberg, and Glauber [34], who employed QED to investigate the fluorescence triplet in a colored vacuum. Specifically, Keitel *et al.*, found that the linewidth of the triplet's central component only depended on the vacuum spectral density at the Rabi sidebands.

V. SUMMARY

Given the history of past attempts to describe spontaneous emission semiclassically, I wish to emphasize that the purpose of the present work is *not* to propound some rival to QED. It has been known for decades that if matter is quantized, then consistency dictates quantization of the electromagnetic field [35]. Rather, the purpose of the present work is simply to extend the range of problems that can be addressed through semiclassical methods. Here, a semiclassical description of radiative decay has been incorporated into the density-matrix equations in order to develop a completely

semiclassical methodology for dealing with strong-field/atom interactions in a colored vacuum.

One application of this methodology, which could have *computational* advantages over QED, would be investigations into multiphoton processes taking place in a low- Q cavity, possibly driven by a stochastic field [36]. In this case, the advantage pertains to the complete problem, and not simply to a calculation of vacuum effects. For example, since the stochastic character of a laser is (arguably) most easily modeled by treating the laser as a classical field, and thereby most easily connected to laboratory measurements, consistency would dictate that the vacuum field should also be treated classically in a stochastic-field/atom interaction problem. Treating the vacuum field by using QED, while accurate, necessitates treatment of the stochastic laser as a quantized field, which is not always the simplest approach for this type of problem. In fact, it was the consideration of such problems that prompted our interest in the present work.

Of course, it must be remembered that the present theory is only an approximation to QED, and therefore there are bounds on its range of validity. For example, by limiting our discussion to the two-level atom we have ignored much of the vector nature of spontaneous emission. While this could probably be accommodated within the semiclassical theory, there seems little to be gained at the present time by the added effort. Of greater significance is the present theory's focus on spontaneous decay and the assumption that the atom does not alter the zero-point field's spectral density. Specifically, taking a conservative point of view, we can only expect the semiclassical theory to agree with QED up to second order in the vacuum's perturbation. This in turn implies that the present theory should only be trusted to describe effects associated with second-order vacuum field statistics. Finally, it must be noted that in order to treat radiation-reaction in a simple way, the density-matrix equations were averaged over the vacuum field. As a consequence, the density-matrix treatment presented here is limited to problems that deal with one-time averages of the zpf, and therefore cannot account for processes that are associated with two-time averages, for example, the resonance fluorescence triplet [37].

Before concluding, it seems worthwhile to suggest that the semiclassical methodology discussed here might find application beyond atomic and optical physics. For example, the present approach may prove useful in studying open quantum systems and the issues surrounding quantum decoherence [38]. Complementing quantum-field treatments of this problem, the present semiclassical approach might provide additional insights given its different intuitive appeal. Additionally, one could imagine using the present approach as a template for developing a semiclassical approximation to quantum gravity in order to study processes associated with the gravitational vacuum. In this vein, it is worth citing the work of Ross and Moreau [39], who have discussed the characteristics of a classical, gravitational zero-point field in the context of an approximation to the real gravitational vacuum. Though both these possible applications of the present work are highly speculative, they do highlight the

benefits to be gained by extending semiclassical methodologies as far as possible.

ACKNOWLEDGMENT

This work was supported under U.S. Air Force Contract No. F04701-93-C-0094.

APPENDIX

In Ref. [14], the Schrödinger equation for an atom interacting with the zero-point field (zpf) of Eq. (3) and its own radiation-reaction field [i.e., Eq. (7)] was solved up to second order in perturbation theory. In typical fashion, the atomic wave function $|\varphi\rangle$ was expanded in terms of eigenfunctions of the unperturbed Hamiltonian $|n\rangle$ and the evolution of the expansion coefficients (or wave-function amplitudes) $a_n(t)$, under the influence of the two field-atom interactions was derived. Specifically, using overbars in this appendix to indicate an average over the zpf, it was found that

$$|\bar{\varphi}\rangle = \sum_n \bar{a}_n(t) e^{-i\omega_n t} |n\rangle, \quad (\text{A1})$$

with \bar{a}_n the sum of a zpf term, \bar{a}_n^{zpf} and a radiation-reaction term \bar{a}_n^{RR} such that

$$\bar{a}_n^{\text{RR}} = -\frac{\bar{a}_n}{3\hbar c^3} \sum_p |\mu_{np}|^2 \omega_{np}^3, \quad (\text{A2a})$$

$$\bar{a}_n^{\text{zpf}} = -\frac{\bar{a}_n}{3\hbar c^3} \sum_p |\mu_{np}|^2 \times \begin{cases} \omega_{np}^3, & \omega_n \geq \omega_p \\ \omega_{pn}^3, & \omega_n \leq \omega_p \end{cases}. \quad (\text{A2b})$$

Of significance is the fact that the two rate terms interfere constructively to produce spontaneous decay, and interfere destructively to inhibit spontaneous excitation.

In order to create a density-matrix that includes this constructive/destructive interference aspect of the atom's interaction with the zpf and its own radiation-reaction field, we would need to employ the zpf-averaged wave function of Eq. (A1):

$$\rho^{(1)} \equiv |\bar{\varphi}\rangle\langle\bar{\varphi}| = \sum_{mn} \bar{a}_m \bar{a}_n^* e^{-i\omega_{mn} t} |m\rangle\langle n|. \quad (\text{A3})$$

Then, for a two-level atom it is straightforward to show that in a rotating frame, where $\rho_{ij} = \sigma_{ij} e^{-i\omega_{ij} t}$,

$$\dot{\sigma}^{(1)} = \begin{pmatrix} \Gamma \sigma_{22} & -\frac{\Gamma}{2} \sigma_{12} \\ -\frac{\Gamma}{2} \sigma_{21} & -\Gamma \sigma_{22} \end{pmatrix}. \quad (\text{A4})$$

Here, Γ is the spontaneous decay rate (i.e., $4|\mu_{21}|^2 \omega_{21}^3 / 3\hbar c^3$), and we have normalized the density matrix. (Since the radiation-reaction perturbation of Ref. [14] is non-Hermitian, population from the excited state is lost unless the requirement of normalization is imposed on the density matrix.) As is obvious from Eq. (A4), construction of the

density matrix from the zpf-averaged wave function yields the proper spontaneous decay behavior.

In a density-matrix treatment of stochastic processes, however, it is customary to employ the atomic wave functions prior to stochastic averaging. The ensemble average behavior of the atomic system is then obtained by averaging the density-matrix elements over the stochastic process [40]. In this fashion, which is essentially that of the present work, we obtain

$$\rho^{(2)} \equiv |\varphi\rangle\langle\varphi| = \sum_{mn} \overline{a_m a_n^*} e^{-i\omega_{mn}t} |m\rangle\langle n|, \quad (\text{A5})$$

or in the rotating frame

$$\sigma^{(2)} \equiv |\varphi\rangle\langle\varphi| = \sum_{mn} \overline{a_m a_n^*} |m\rangle\langle n|. \quad (\text{A6})$$

The problem with $\sigma^{(2)}$ for describing spontaneous emission semiclassically is that the constructive/destructive interference aspects of the zpf and radiation-reaction perturbations will not be manifested in the $\overline{a_m a_n^*}$ terms if the perturbations of Ref. [14] are employed. Basically, if we are to inhibit spontaneous excitation through the interference mechanism, then we need to average over the wave-function amplitudes and not the probabilities for an atom being in a specific state.

An expedient solution to this density-matrix averaging ambiguity lies in the fact that the radiation-reaction perturbation is not gauge invariant, which implies that it is only a computational tool. Therefore, we have some liberty to define this perturbation so as to make the evolution of $\sigma^{(2)}$ consistent with the evolution of $\sigma^{(1)}$. Considering for the

moment just the diagonal components of the density matrix $\sigma^{(2)}$, we can write their evolution as the sum of a zpf-induced evolution and a radiation-reaction evolution:

$$\dot{\sigma}_{ii}^{(2)} = \dot{a}_i^{\text{zpf}} a_i^* + \dot{a}_i^{\text{RR}} a_i^* + c.c.. \quad (\text{A7})$$

We then employ our freedom on the form of the radiation-reaction perturbation to write $\dot{a}_1^{\text{RR}} a_1^* = -\dot{a}_1^{\text{zpf}} a_1^*$ and $\dot{a}_2^{\text{RR}} a_2^* = \dot{a}_2^{\text{zpf}} a_2^*$, which is just the ansatz of Eq. (9). In this way, spontaneous excitation of the ground state is inhibited while spontaneous decay of the excited state proceeds with the proper rate.

In order to show that the above choice of radiation-reaction evolution leads back to Eq. (A4), we can consider Eqs. (26) in the case of free space, where $\eta = 2/3$. In that situation, since the sum over zpf modes will be dominated by terms with $\delta_s = 0$, we can let $\omega_s \rightarrow \omega_{21}$ so that

$$\dot{\sigma}_{12}^{(2)} = -\frac{\Gamma}{2\pi} \int_0^t \sigma_{12}^{(2)}(t') \sum_{s=0}^{\infty} e^{i\delta_s(t-t')} \Delta\omega_s dt', \quad (\text{A8a})$$

$$\dot{\sigma}_{22}^{(2)} = -\frac{\Gamma}{\pi} \int_0^t \sigma_{22}^{(2)}(t') \sum_{s=0}^{\infty} \cos[\delta_s(t-t')] \Delta\omega_s dt'. \quad (\text{A8b})$$

Changing the sum over modes to an integral, and ignoring terms associated with the Lamb shift, Eqs. (A8) yield $\dot{\sigma}_{12}^{(2)} = -\frac{1}{2}\Gamma\sigma_{12}^{(2)}$ and $\dot{\sigma}_{22}^{(2)} = -\Gamma\sigma_{22}^{(2)}$, which with normalization yields a density-matrix evolution that is equivalent to the $\dot{\sigma}^{(1)}$ of Eq. (A4).

-
- [1] J. N. Dodd, *Atoms and Light: Interactions* (Plenum, New York, 1991).
- [2] G. W. Series, *Phys. Rep.* **43**, 1 (1978).
- [3] W. Happer, *Rev. Mod. Phys.* **44**, 169 (1972).
- [4] A. T. Georges and P. Lambropoulos, *Adv. Electron. Electron Phys.* **54**, 191 (1980).
- [5] See, for example, W. Heitler, *The Quantum Theory of Radiation* (Dover, New York, 1984), Sec. 18.
- [6] P. Lambropoulos, G. M. Nikolopoulos, T. R. Nielsen, and S. Bay, *Rep. Prog. Phys.* **63**, 455 (2000).
- [7] R. K. Lee, O. J. Painter, B. Kitzke, A. Scherer, and A. Yariv, *Electron. Lett.* **37**, 569 (1999); J.-K. Hwang, H.-Y. Ryu, D.-S. Song, I.-Y. Han, H.-W. Song, H.-K. Park, and Y.-H. Lee, *Appl. Phys. Lett.* **76**, 2982 (2000).
- [8] M. O. Scully and M. S. Zubairy, *Quantum Optics* (Cambridge University Press, Cambridge, 1997), Chap. 5.
- [9] P. W. Milonni, *Phys. Rep.* **25**, 1 (1976).
- [10] See for example: A. G. Redfield, *IBM J. Res. Dev.* **1**, 19 (1957); P. R. Berman, *J. Opt. Soc. Am. B* **3**, 564 (1986), and references therein.
- [11] See, for example, J. N. Dodd, *Phys. Scr.* **T70**, 88 (1997).
- [12] See: T. H. Boyer, in *Foundations of Radiation Theory*, edited by A. O. Barut (Plenum, New York, 1980), and references therein; also, T. W. Marshall, *Proc. R. Soc. London, Ser. A* **276**, 475 (1963); and R. Bourret, *Phys. Lett.* **12**, 323 (1964).
- [13] I. R. Senitzky, *Phys. Rev. Lett.* **31**, 955 (1973); P. W. Milonni, J. R. Ackerhalt, and W. A. Smith, *ibid.* **31**, 958 (1973).
- [14] J. C. Camparo, *J. Opt. Soc. Am. B* **16**, 173 (1999).
- [15] W. H. Louisell, *Quantum Statistical Properties of Radiation* (Wiley, New York, 1973), pp. 336–344; K. Blum, *Density Matrix Theory and Applications* (Plenum, New York, 1981), Chap. 7.
- [16] D. J. Heinzen and M. S. Feld, *Phys. Rev. Lett.* **59**, 2623 (1987).
- [17] C. H. Keitel, P. L. Knight, L. M. Narducci, and M. O. Scully, *Opt. Commun.* **118**, 143 (1995).
- [18] We note that this approach is somewhat different from that taken in Ref. [14], where the radiation-reaction field was formulated as an Hermitian atomic operator. In that case, the electric dipole perturbation on the atom was a non-Hermitian operator.
- [19] J. Dalibard, J. Dupont-Roc, and C. Cohen-Tannoudji, *J. Phys. (Paris)* **43**, 1617 (1982).
- [20] C. Cohen-Tannoudji, B. Diu, and F. Laloë, *Quantum Mechanics: Volume 1* (Wiley, New York, 1977), pp. 315–328.
- [21] R. R. Schlicher, W. Becker, J. Bergou, and M. O. Scully, in *Quantum Electrodynamics and Quantum Optics*, edited by A. O. Barut (Plenum, New York, 1984), pp. 405–441.

- [22] P. W. Milonni, *The Quantum Vacuum: An Introduction to Quantum Electrodynamics* (Academic, Boston, 1994).
- [23] H. B. Callen and T. A. Welton, Phys. Rev. **83**, 34 (1951).
- [24] P. W. Milonni, Phys. Scr., **T21**, 102 (1988).
- [25] J. C. Slater, *Quantum Theory of Matter* (McGraw-Hill, New York, 1951), Chap. 6.
- [26] In performing the ensemble average (i.e., $\langle \dots \rangle$) we average the zpf modes over their possible amplitudes. Here, we average the zpf modes over their possible propagation directions in space.
- [27] Though Heinzen and Feld imply a mirror reflectivity of 0.65 for their étalon, they state that best agreement between theory and experiment suggested $R=0.5$. This latter value was used in the calculations of the present work. Additionally, as Heinzen and Feld do not provide an absolute reference for their cavity's tuning, this is a free (though insignificant) parameter in the fit between theory and experiment shown in Fig. 2.
- [28] S. Niggli and M. C. E. Huber, Phys. Rev. A **35**, 2908 (1987); **37**, 2714(E) (1988); **39**, 3924 (1989).
- [29] Since the density-matrix equations were derived by ensemble averaging over the zpf, it is not possible to calculate the fluorescent triplet with the present theory. In order to calculate the ac Stark doublet, it would be necessary to augment the present theory's two-level density matrix with a third state. In principle, this should be straightforward.
- [30] M. W. Hamilton, K. Arnett, S. J. Smith, D. S. Elliot, M. Dzeimballa, and P. Zoller, Phys. Rev. A **36**, 178 (1987); A. T. Georges and P. Lambropoulos, *ibid.* **18**, 587 (1978).
- [31] J. C. Camparo and P. Lambropoulos, Phys. Rev. A **47**, 480 (1993).
- [32] R. H. Pennington, *Introductory Computer Methods and Numerical Analysis* (MacMillan, London, 1970), Chap. 11.
- [33] A. Papoulis, *The Fourier Integral and Its Applications* (McGraw-Hill, New York, 1962).
- [34] M. Lewenstein, T. W. Mossberg, and R. J. Glauber, Phys. Rev. Lett. **59**, 775 (1987).
- [35] W. Heitler, *The Quantum Theory of Radiation* (Dover, New York, 1984), Sec. 9.
- [36] For examples of stochastic-field effects and multiphoton processes in free space, see J. C. Camparo and P. Lambropoulos, Phys. Rev. A **59**, 2515 (1999), and references therein.
- [37] M. O. Scully and M. S. Zubairy, *Quantum Optics* (Cambridge University Press, Cambridge, 1997), Chap. 10.
- [38] W. H. Zurek, Phys. Today **44** (10), 36 (1991); D. Giulini, E. Joos, F. Kiefer, J. Kupsch, I. O. Stamatescu, and H. D. Zeh, *Decoherence and the Appearance of a Classical World in Quantum Theory* (Springer, Berlin, 1996).
- [39] D. K. Ross and W. Moreau, Gen. Relativ. Gravit. **27**, 845 (1995).
- [40] See, for example, C. P. Slichter, *Principles of Magnetic Resonance* (Harper & Row, New York, 1963), Chap. 5.

LABORATORY OPERATIONS

The Aerospace Corporation functions as an "architect-engineer" for national security programs, specializing in advanced military space systems. The Corporation's Laboratory Operations supports the effective and timely development and operation of national security systems through scientific research and the application of advanced technology. Vital to the success of the Corporation is the technical staff's wide-ranging expertise and its ability to stay abreast of new technological developments and program support issues associated with rapidly evolving space systems. Contributing capabilities are provided by these individual organizations:

Electronics and Photonics Laboratory: Microelectronics, VLSI reliability, failure analysis, solid-state device physics, compound semiconductors, radiation effects, infrared and CCD detector devices, data storage and display technologies; lasers and electro-optics, solid state laser design, micro-optics, optical communications, and fiber optic sensors; atomic frequency standards, applied laser spectroscopy, laser chemistry, atmospheric propagation and beam control, LIDAR/LADAR remote sensing; solar cell and array testing and evaluation, battery electrochemistry, battery testing and evaluation.

Space Materials Laboratory: Evaluation and characterizations of new materials and processing techniques: metals, alloys, ceramics, polymers, thin films, and composites; development of advanced deposition processes; nondestructive evaluation, component failure analysis and reliability; structural mechanics, fracture mechanics, and stress corrosion; analysis and evaluation of materials at cryogenic and elevated temperatures; launch vehicle fluid mechanics, heat transfer and flight dynamics; aerothermodynamics; chemical and electric propulsion; environmental chemistry; combustion processes; space environment effects on materials, hardening and vulnerability assessment; contamination, thermal and structural control; lubrication and surface phenomena.

Space Science Applications Laboratory: Magnetospheric, auroral and cosmic ray physics, wave-particle interactions, magnetospheric plasma waves; atmospheric and ionospheric physics, density and composition of the upper atmosphere, remote sensing using atmospheric radiation; solar physics, infrared astronomy, infrared signature analysis; infrared surveillance, imaging, remote sensing, and hyperspectral imaging; effects of solar activity, magnetic storms and nuclear explosions on the Earth's atmosphere, ionosphere and magnetosphere; effects of electromagnetic and particulate radiations on space systems; space instrumentation, design fabrication and test; environmental chemistry, trace detection; atmospheric chemical reactions, atmospheric optics, light scattering, state-specific chemical reactions and radiative signatures of missile plumes.

Center for Microtechnology: Microelectromechanical systems (MEMS) for space applications; assessment of microtechnology space applications; laser micromachining; laser-surface physical and chemical interactions; micropropulsion; micro- and nanosatellite mission analysis; intelligent microinstruments for monitoring space and launch system environments.

Office of Spectral Applications: Multispectral and hyperspectral sensor development; data analysis and algorithm development; applications of multispectral and hyperspectral imagery to defense, civil space, commercial, and environmental missions.